

# Getting more out of drillhole televiewer data: geotechnical toolbox edition

**J Danielson** BGC Engineering, Canada

**MA Clayton** BGC Engineering, Canada

**L Kelly** BGC Engineering, Canada

**D Kinakin** BGC Engineering, Canada

## Abstract

*This paper presents three case studies that utilise acoustic televiewer (ATV) survey data to improve the quality and consistency of geomechanical parameters including intact rock strength, joint condition, fracture spacing and rock mass quality. Two methods of leveraging televiewer data for geomechanical characterisation are explored. The first method employs scripted generation of downhole plots which compare average acoustic amplitude and travel time against logged strength and joint condition. The second is a preliminary automated structure identification workflow built on a state-of-the-art computer vision model (YOLOv8) trained to identify open discontinuities. Rock quality designation (RQD) and fracture count are estimated from the model outputs.*

*Case study 1 illustrates an example of how these automated tools can be used to assist in maintaining data quality and consistency across large teams. It highlights the close correlation between acoustic amplitude and logged strength grade, and between travel time and joint condition, and demonstrates how these relationships can be used to identify logging errors and areas of improvement for individual loggers. Case 2 describes a multi-year drilling program where ATV data were used to improve confidence in logged strengths across weathering horizons and demonstrates a particularly strong relationship between acoustic amplitude and Leeb hardness. Case 3 evaluates the performance of the automated structure identification workflow when used for estimating RQD and fracture count, highlighting the tool's strengths and limitations. These cases demonstrate ATV data's significant potential for improving the consistency and quality of geotechnical characterisation.*

**Keywords:** televiewer data, rock mass characterisation, quality assurance, artificial intelligence

## 1 Introduction

The survey data collected by acoustic and optical borehole televiewers has dramatically changed the landscape of geological and geotechnical subsurface structural data collection over the last 15 years. It is now relatively easy and low cost to collect thousands of metres of downhole structural measurements, and many mine owners, geotechnical consultants and exploration groups have adopted televiewer imaging as part of their standard toolbox. As a result, many sites have accumulated a substantial library of televiewer data. This data presents a challenge and an opportunity because on the one hand, processing the data manually is time-consuming and therefore expensive, and on the other, the mining industry has never before had access to so much high-quality downhole data that can be independently verified. There is also the opportunity to explore additional uses for the data to validate geotechnical input parameters essential to slope stability analyses including intact strength and fracture frequency, and to make use of recent advances in machine learning and digital image analysis to streamline the process.

High quality core logging data is critical for the successful design and management of open pit slopes. Physical logging, data processing and quality assurance of geomechanical data represents a huge cost, whether completed by in-house staff or by engineering consultants. However, despite best efforts to collect

high-quality data, consistency issues are pervasive; in part because logging staff change across shifts, programs and years. As a result, data quality can suffer, leading to further expense and/or delays during the design process. Problems not immediately discovered can require re-evaluation of already-completed analyses or contribute to inappropriate designs.

Given these challenges there is a need to improve geotechnical drilling data consistency and to validate the quality of data collected by others. But check logging, particularly when only photos are available, is time-consuming and often not practical for large quantities of data. Televiewer data represents a promising avenue for quality assurance. It exists in a digital format, is often available in large quantities and offers a level of consistency unattainable with other data sources. The potential of televiewer data is further amplified by recent advancements in programming and machine-learning techniques, which provide the capacity to quickly process large amounts of data and generate comparisons with core logging data. This paper presents three case studies that explore strategies for leveraging televiewer data to improve geomechanical characterisation and logging quality. Through this exploration, the authors aim to demonstrate the potential of these techniques to improve geotechnical data quality and consistency in the mining industry.

## 2 Data and methods

Acoustic televiewers (ATVs) create images of subsurface rock by emitting acoustic waves and recording the reflections of those waves (Zemanek et al. 1970). The two most important parameters describing the reflections are amplitude, which describes the intensity of the reflected wave, and travel time, which is the time taken for the reflected wave to return to the probe (Figure 1). Televiewer imagery is most frequently used to identify and measure the orientation of discontinuities like joints, faults and veins. Its use in geomechanical characterisation has been explored (Kao et al. 2020; Dempers et al. 2019) but is not widespread.

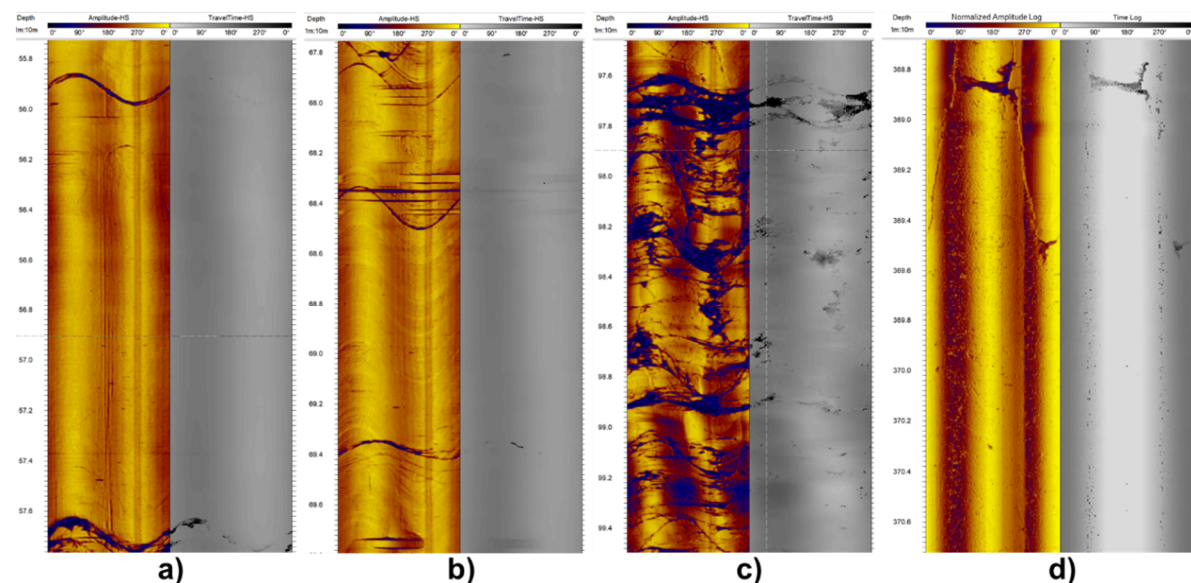


**Figure 1** ATV log data examples showing amplitude (left) and travel time (right): (a) Massive rock with few distinct discontinuities; (b) Interbedded fine and coarse sediments with few distinct discontinuities; (c) Highly fractured rock mass containing weak shale beds; (d) Texture and upper contact of an intrusive body

One benefit of televiewer data is that it provides relatively high-resolution data along the length of hole surveyed. In contrast to point load or field strength estimates, which are commonly collected every one to three metres, amplitude and travel time data are typically collected along 144 points around the drillhole wall every 3–4 mm.

## 2.1 Acoustic amplitude

Acoustic amplitude depends on the acoustic impedance contrast between the drillhole fluid and the drillhole wall. Harder rock has higher acoustic impedance and softer rock has lower acoustic impedance. Tests on cement show a strong and linear relationship between compressive strength and acoustic impedance at the range of 5 to 50 MPa (Bu et al. 2011). Acoustic amplitude is conceptually similar to rebound from tests like the Schmidt hammer or Leeb hardness tests (Seguin et al. 2022), which measure magnitude of reflected energy, except that the energy is in the form of a sound wave instead of a physical mass. Acoustic amplitude and physical rebound tests share some limitations. Both may be sensitive to porosity, roughness of the surface being tested and scale effects, and relationships can vary between lithologies and rock types.

Despite these limitations, acoustic amplitude shows a strong relative relationship with rock strength. Figure 2 shows violin plots with the estimated distribution of amplitude values for each logged International Society for Rock Mechanics (ISRM) strength grade for two drillholes. Horizontal lines show the maximum, median and minimum value within each distribution, and 'n' shows the number of logged intervals represented in each distribution. The amplitude distributions show a clear increasing relationship with rock strength. In terms of a relative relationship, the amplitude-strength relationship is impressive, especially given the imprecise nature of field strength estimates, ambiguity in field strength definitions and differences in interpretation from logger to logger. Amplitude often shows a better relationship with logged strength grade compared to other estimates of strength like point load testing, which show considerable scatter (Figure 3). Nevertheless, the absolute amplitude between holes is quite different: in Figure 2, the amplitudes from the first drillhole are nearly an order of magnitude higher at the same strength grade. Amplitude can be calibrated to a known value within a drillhole but it is difficult to use as a purely independent check on logged strengths.

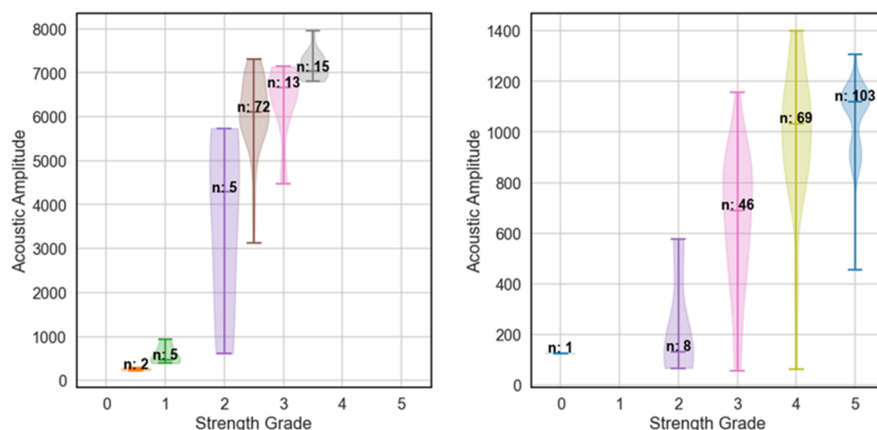


**Figure 2** Acoustic amplitude versus strength grade for two different drillholes

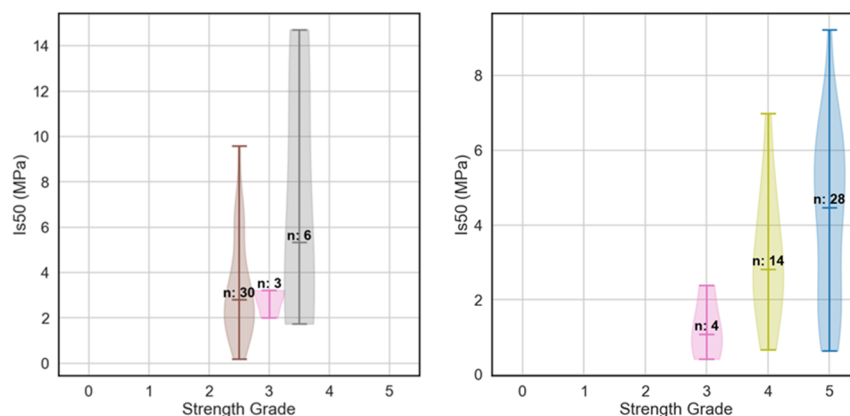


**Figure 3** Is50 distributions from point load testing versus strength grade for the same drillholes. Note the wider distributions and weaker relationship compared with amplitude from the same drillholes

Hole-to-hole differences in amplitude depend not only on the wall rock but also on the specific televiewer instrument used, the drillhole fluid and any coating on the drillhole walls. A drop in amplitude unrelated to rock strength is typically seen at the bottom of drillholes where cuttings can accumulate in the fluid column and along the drillhole wall. Figure 4 shows an example of this behaviour in the bottom 16 m of a 500 m-deep hole, showing amplitude plotted as an image and mean amplitude plotted as a white line. Amplitude should not be used for inferring strength near hole bottoms.

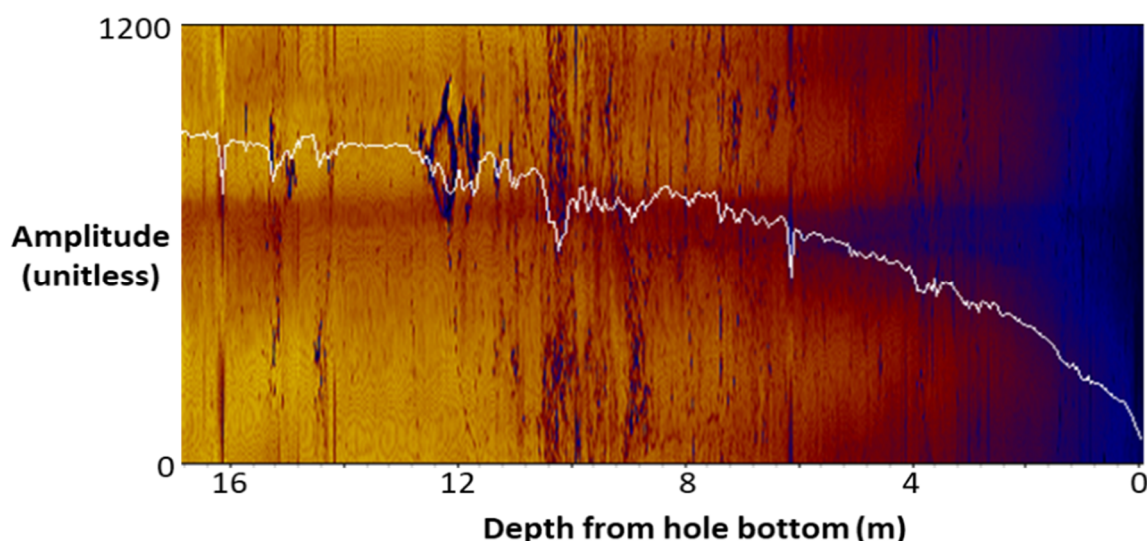


**Figure 4** The decrease in amplitude approaching the bottom of a deep hole

When inferring strength or other geomechanical characteristics from amplitude, practitioners should avoid using normalised logs. The normalisation routines available in well log processing software improve the local contrast within the image and help highlight discontinuities but reduce the interval-scale differences in the amplitude of intact rock.

## 2.2 Acoustic travel time

Acoustic travel time is indicative of the distance between the drillhole wall and the televiewer probe. An assumption of the speed of sound in the borehole fluid can be used to estimate the drillhole diameter ('acoustic calliper'). It highlights open discontinuities, breakouts and areas where softer material has washed away during drilling. It is particularly useful for highlighting geotechnically important features. Travel time also depends on factors unrelated to features of interest, like the speed of sound in the hole fluid and the diameter of the drillhole, which can vary slightly with drill bit wear. Plotting 'enlargement', the difference between the maximum and average travel time at each given depth, avoids these issues and better highlights features of interest compared with raw travel time or raw acoustic calliper (Figure 5).



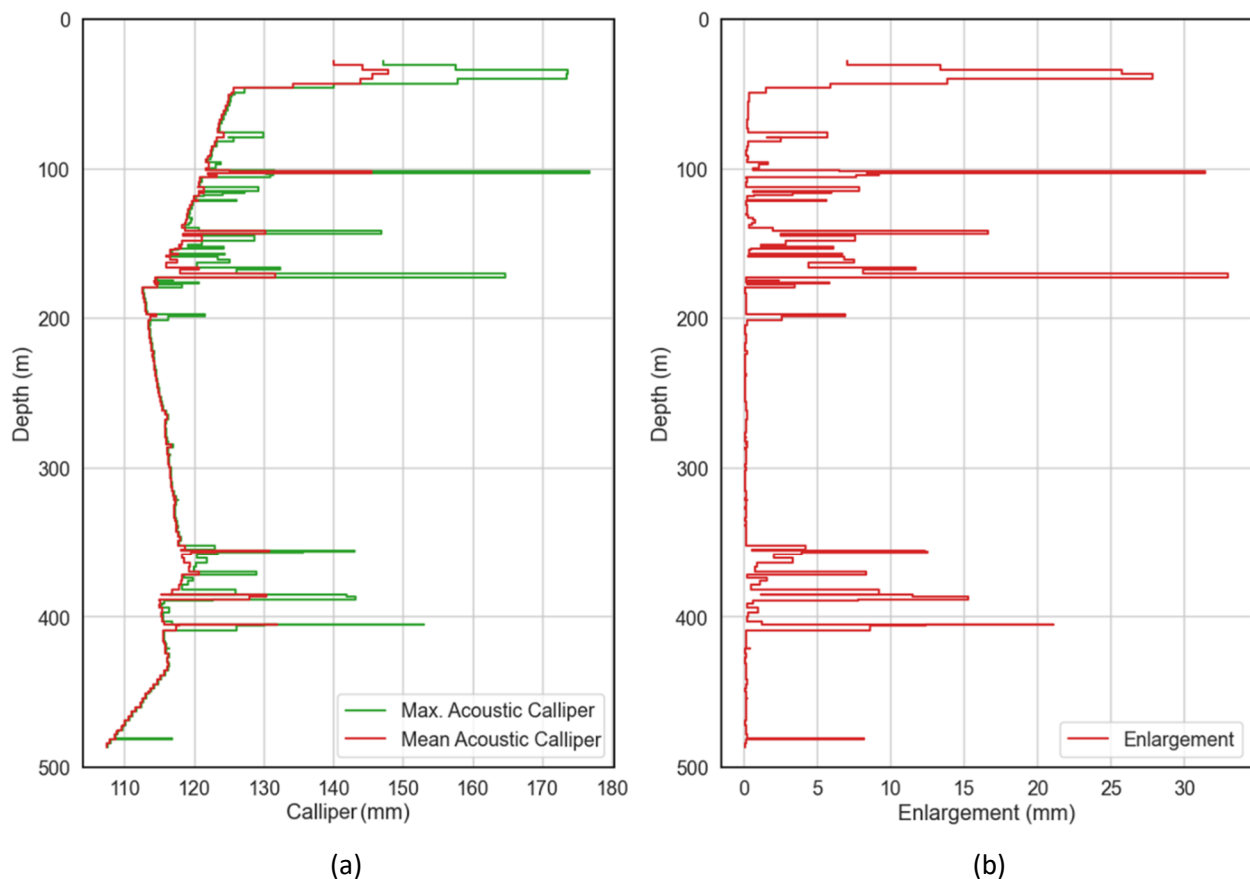


**Figure 5** Acoustic calliper from travel time (a) and enlargement (b) with depth for an example drillhole

### 2.3 Automated structure logging

Estimating geomechanical parameters from televiewer structure logs is challenging. Loggers can be inconsistent about the scale of features logged and whether discontinuous, flat or intact features (like bedding or foliation without an actual separation) are logged. Automated structure logging from televiewer data has the potential to improve some of these consistency issues.

Recent advancements in computer vision technology have provided techniques to identify and segment objects for applications like augmented reality, intelligent driving, and medical image analysis (Gu et al. 2022). These techniques have also been applied to the geotechnical and structural interpretation of core photos (Alzubaidi et al. 2022a, 2022b, 2023). This paper explores an automated workflow that utilises a preliminary YOLOv8 instance segmentation model (Jocher et al. 2023) trained on a relatively small dataset, comprising approximately 110 m of televiewer data, to identify and characterise the aperture of structures. The model was trained on approximately 320 manually labelled features judged to be open and continuous around the circumference of the borehole. During the training phase the data was divided into training and validation datasets, with approximately 90% of the data used for training and the remaining 10% set aside to evaluate the model's performance.

Model performance can be gauged using the mean average precision (mAP) score. This score is derived from the number of structures that the model correctly predicts ('true positives'), the number of structures that were predicted but were not associated with a manually labelled feature ('false positives') and the number of structures missed by the model ('false negatives'). Higher mAP scores indicate better performance; a score of 1.0 would signify that all structures were identified correctly with no false positives or false negatives. The trained model used in this paper achieved a mAP score of 0.90 against the validation dataset, considering an overlap of at least 50% between the manually labelled and predicted features.

The instance segmentation model takes images as inputs. To develop suitable image inputs from the ATV data, travel time is set as the red channel for the image, and acoustic amplitude is used as the basis for the blue and green channels of the image. Example image inputs and identified structures from a drillhole separate from those used in training the model are shown in Figure 6. Sine wave fitting and location calculations are modified from work by Alzubaidi et al. (2022b). Cases 1 and 3 explore the potential to estimate rock quality designation (RQD) and fracture frequency based on the estimated location and apertures of the identified structures.

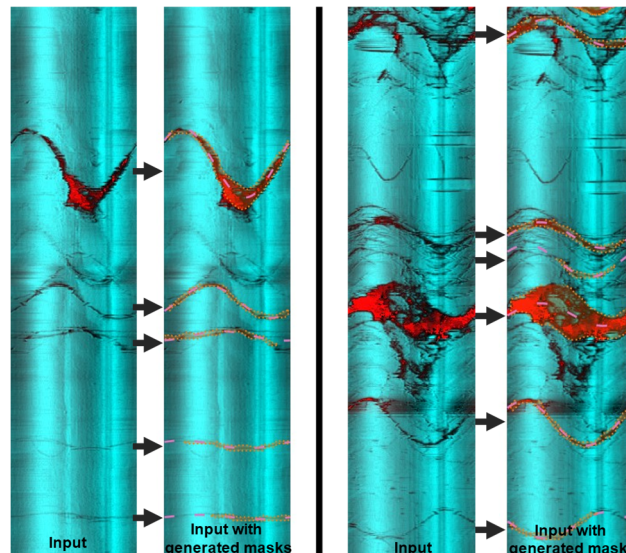


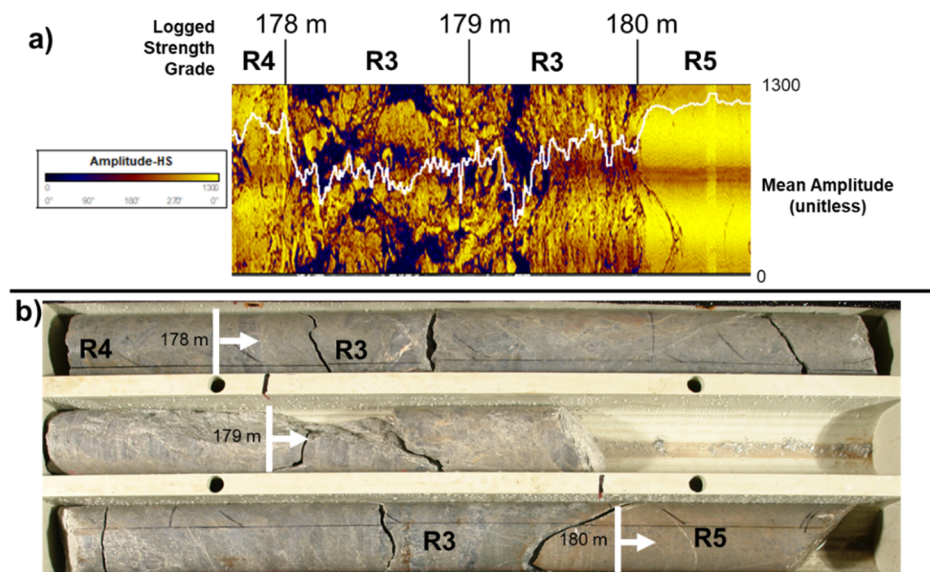
**Figure 6 Two examples of televiewer data processed using the automated structure logging workflow. Each example shows the image input and overlain model-generated segmentation masks (filled dotted orange lines) and fitted sine waves (pink dashed lines)**

Workflows and machine-learning models have important limitations. They require site-specific validation, and interpretation of results should always include checks against core photos and other data sources. Models may not generalise to conditions greatly different than those used in model training. If model performance at a new site is poor, a small training dataset may be sufficient to fine-tune the existing model to new conditions. The authors intend to continue developing processing tools and adding to the training dataset to broaden the applicability and usefulness of these methods.

### 3 Case 1

Case 1 involved an experienced client team performing in-house geotechnical and geophysical logging. Both geotechnical and geophysical logging were high quality. However, the team was large, which required rapid data validation and quality assurance (QA) to maintain consistency across different shifts and rotations. In response, BGC developed an automated tool to generate downhole plots of geotechnical parameters and ATV data once the data were available for each drillhole. Acoustic amplitude was plotted against field estimated strength, and acoustic enlargement against joint condition. Because of the high resolution of the data and because strength is variable at a small scale, raw data can appear noisy. To mitigate this, binned median amplitude was plotted over intervals aligned with those from core logging.

At this site, amplitude served as a suitable QA check on the logged strength grade. Acoustic amplitude displayed a close relative correlation with field strength, where drops in amplitude were associated with drops in strength grade and increases in amplitude were associated with increases in strength grade (Figure 7).



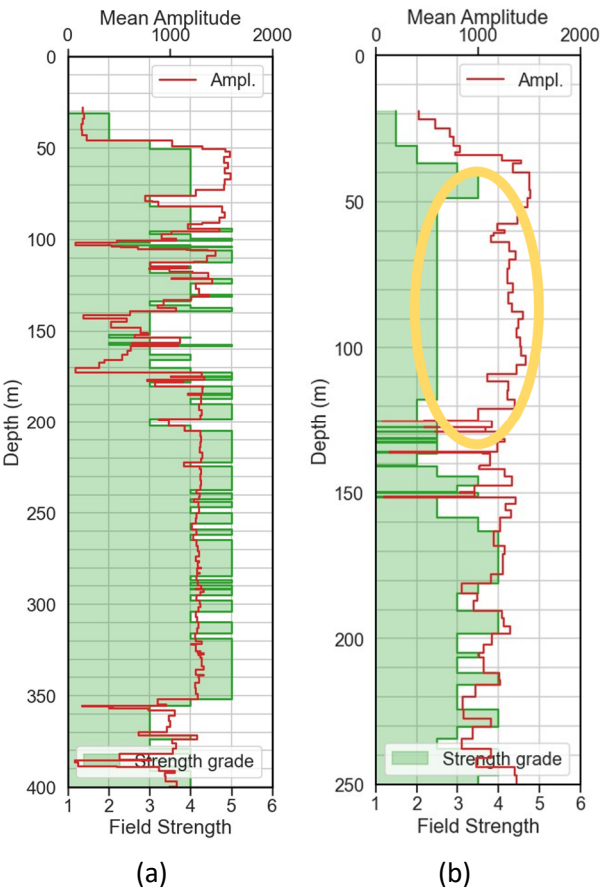
**Figure 7 (a) Amplitude image and average (shown as white line) compared with logged strengths; (b) The core photo for the same depths**

Figure 8 illustrates automatically generated amplitude and strength plots versus depth for two drillholes. The first hole shows a strong relationship between amplitude and strength grade. The second shows a reasonable relationship between amplitude and strength but highlights an area in the first half of the drillhole where logged strength grade appears unusually uniform and lower than strength grades logged for similar amplitudes deeper in the same hole. This plot could be used as a basis for re-logging or a targeted review of strength grade procedures with the logger responsible for the anomalous result.

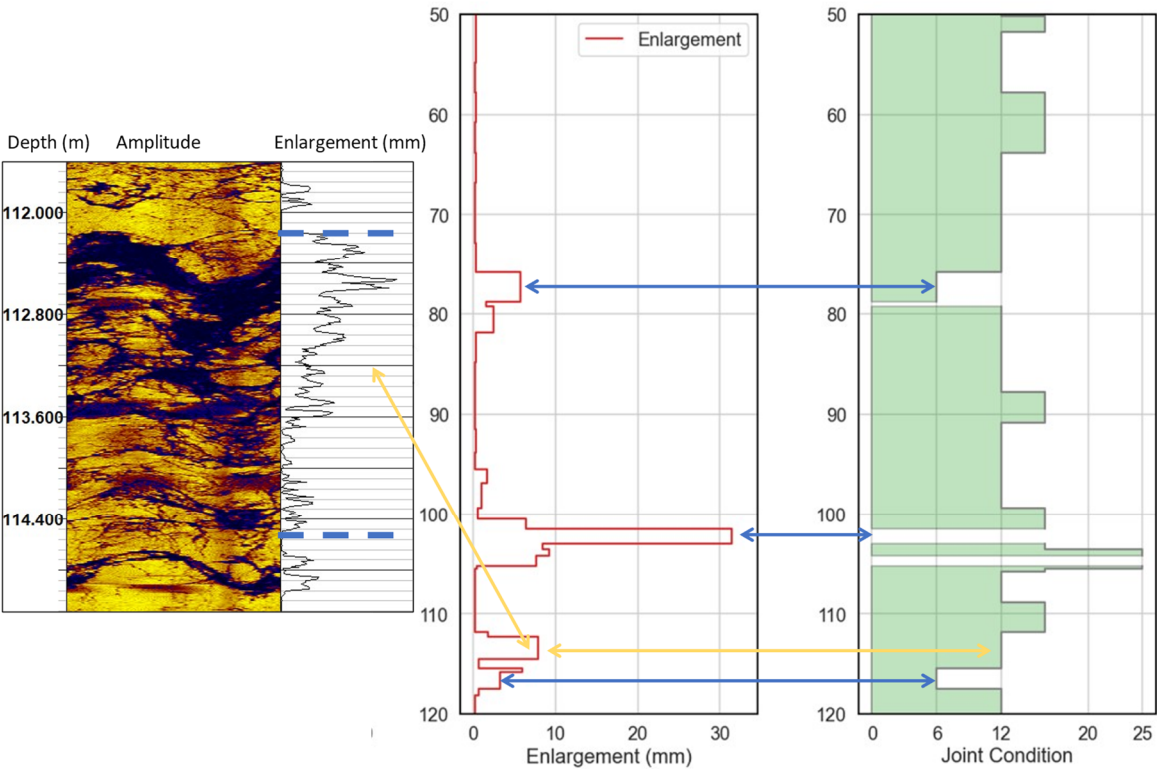
Enlargement tends to highlight large open discontinuities or discontinuities with infill soft enough to erode during drilling. These types of discontinuities are often the most geotechnically important. At this site, enlargements greater than approximately 5 mm typically correlate with low RMR76 (Bieniawski 1976) joint conditions (six or lower). Figure 9 shows three examples (blue arrows) showing where this is observed and enlargement is associated with a drop in joint condition. It also highlights one interval (yellow arrow) where logged joint condition was 12, but inspection of the ATV log and core photos indicates logged joint condition should have been six or lower. While enlargement can be caused by conditions unrelated to joint condition, like stress-induced breakouts, these conditions are relatively rare at this site. Enlargement serves as a useful identifier for highlighting overestimated joint condition and potentially overlooked geotechnically important features.

Figure 10 shows a comparison between RQD and fracture frequency measured by experienced loggers and automatically estimated from the automated structure logging workflow (Section 2.3). Discontinuity counts match relatively well, particularly in the bottom half of the drillhole. Review of the automated workflow structure picks indicates a very low rate of false positives (approximately 3%) but a false negative rate (missed structures) of approximately 20%. Manually and automatically logged counts consider crushed rock and wide aperture zones similarly, where additional discontinuities are added for every centimetre of soft or crushed infill. RQD estimates from the workflow are higher than logged estimates, which may be partially due to loggers not measuring over mechanical breaks and partially due to limitations in the workflow.

Case 1 demonstrates how geophysical data can improve the quality of logging data. Although the geophysical parameters considered can be affected by factors unrelated to geotechnical parameters of interest and cannot be used to directly estimate geotechnical parameters, their 'strong enough' relationships with geotechnical parameters make them valuable in improving logging consistency, identifying areas of improvement for individual loggers and highlighting significant features that might otherwise have been overlooked. Because the generation of these plots is automated and uses data already being collected, the additional effort required for generating these plots is negligible, while interpretation of them provides a real benefit.



**Figure 8** Amplitude (unitless) and strength versus depth for two holes showing (a) a typical hole; and (b) a hole where one part of the hole was logged inconsistently



**Figure 9** Enlargement and joint condition

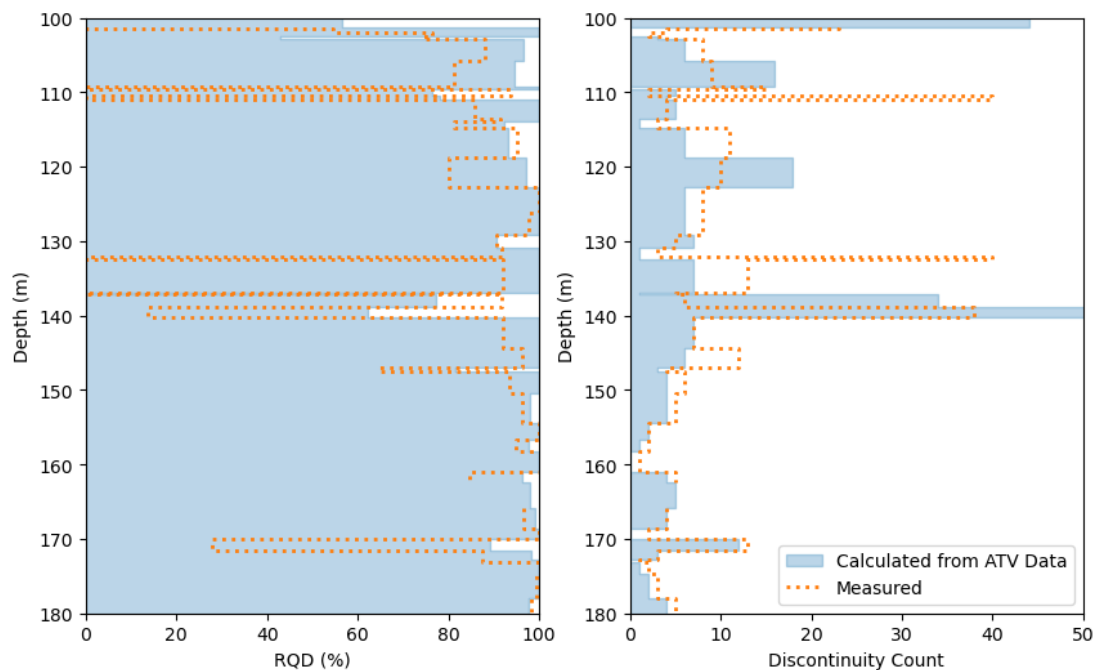


**Figure 10 Automatically estimated RQD and discontinuity counts compared with measured (logged) values. Estimates were made using the same intervals used for manual logging**

## 4 Case 2

Case 2 involved a multi-year drilling program with over 100 geotechnical drillholes advanced through layered volcanic and sedimentary rock units with weathering grades varying from residual soil (W6) to fresh rock (W1). Geomechanical characterisation was conducted over multiple years by the client, the contractor and consultant staff. Televiewer surveys were completed for approximately 50% of the holes drilled and were used as part of the QA process to evaluate the quality of logged geotechnical parameters. Leeb hardness tests were performed at regular intervals along core from some drillholes. Downhole plots were generated to compare acoustic amplitude to logged field strength and Leeb hardness values to verify the quality of the logged strength values reported.

Figure 11 shows a downhole comparison of amplitude, field strength and Leeb hardness. These three measures of strength show a strong correlation in the fresh rock where the ATV data was collected. Zones of weaker rock are observed through proportionally similar decreases in field strength, Leeb hardness and acoustic amplitude, as can be seen from 85–90 m. A decrease in acoustic amplitude is observed at the end of the hole. This is potentially due to the accumulation of cutting and results in a poor correlation to the Leeb hardness and ISRM field strength grade.



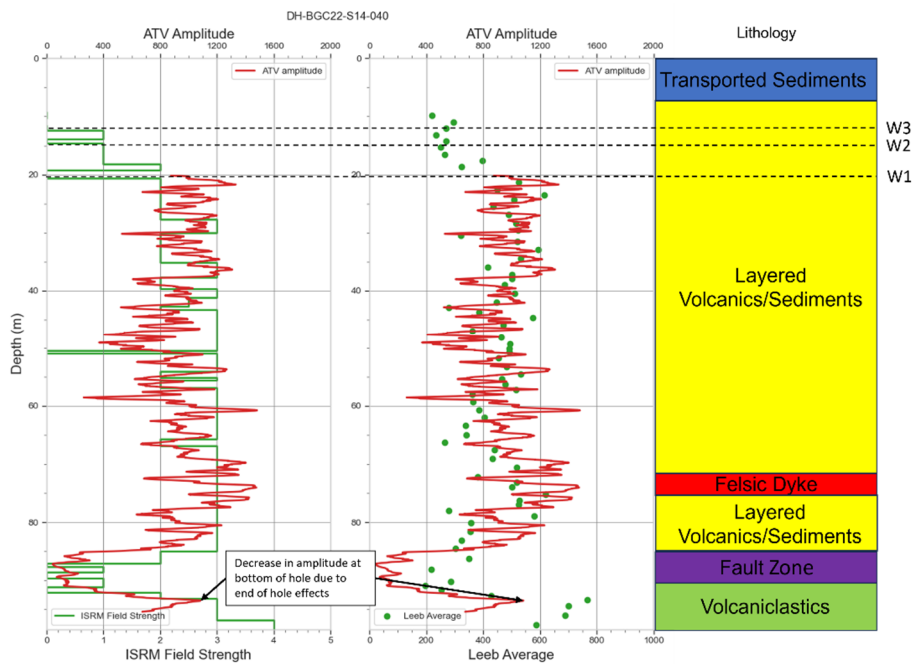


**Figure 11 Comparison of field strength and Leeb hardness value against acoustic amplitude (unitless) for fresh rock**

Figure 12 shows a borehole where ATV data were available below the W3 (moderately weathered) horizon. Amplitude closely correlates with the logged field strength values and the Leeb hardness values across the weathering grades encountered. At a depth of 52 m the amplitude rapidly decreases, but a similar drop is not observed in the logged field strength values. Leeb hardness data is not available at this depth. A review of core photos indicates this section of core is characterised by a zone of highly broken rock with limited core recovery. The logged field strength at this depth was overestimated, as detected by the acoustic amplitude QA process.

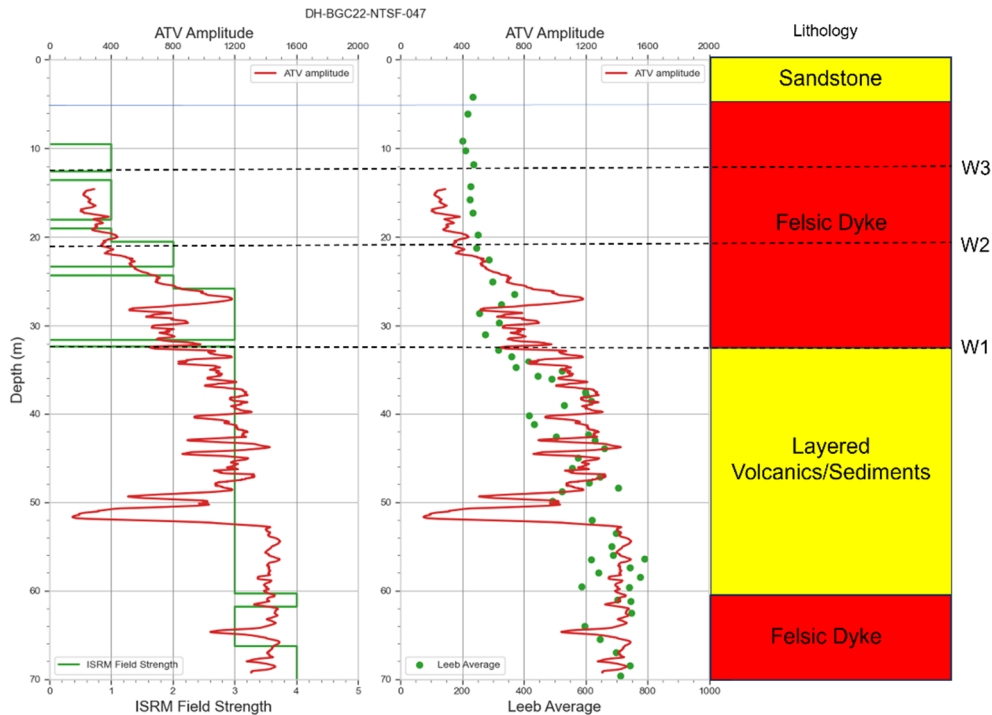


**Figure 12 Comparison of field strength and Leeb hardness value against acoustic amplitude (unitless) for moderately weathered to fresh rock**

In Case 2, the ATV amplitude data provided the ability to rapidly assess the quality of logged strength grades and improve confidence in the values used for future design.

## 5 Case 3

Case 3 is a site with a substantial subsurface site investigation database dating back to 1998 and oriented core drilling has been selectively completed using a variety of methods. Acoustic and optical televiewer surveys were first completed at the site in 2005. Televiewer surveys have been completed as part of standard data collection since 2017 for resource and geotechnical drilling campaigns. The geology of the site is primarily turbidite-dominated deep-water facies sedimentary rocks which have a high degree of compositional variability. The sedimentary rocks range from very strong lithic sandstones (greywacke) to weak graphitic shales. Since 2010, the project has used flysch grades (Figure 13) based on the framework developed by Marinos & Hoek (2000) to characterise the rock mass based on the composition and structure of the interbedded sediments. This framework also provides a method for estimating representative strengths for the compositionally variable material, which has been particularly useful for slope stability assessments.

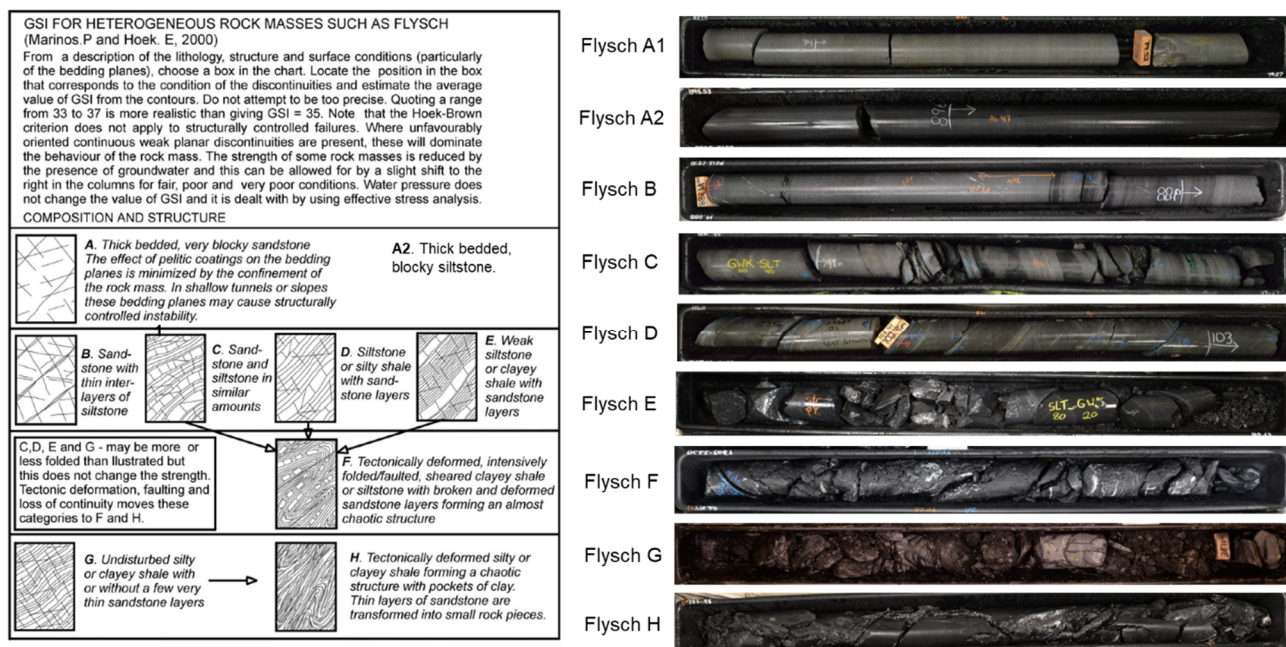


**Figure 13 Flysch grade system (after Marinos & Hoek 2000) and core photo examples**

At this site, BGC recently drilled over 40 short ( $\leq 100$  m) geotechnical holes with televiewer surveys. The authors used the automated structure logging routine described in Section 2.3 to speed up the processing of discontinuity data, which is not discussed in this paper, and evaluate the routine's performance for rapid fracture density and blockiness assessment.

Figure 14 shows an example of RQD and fracture frequency estimated using the automated structure logging routine and a comparison with logged values plotted with relative proportions of greywacke, siltstone and shale. The automated RQD and fracture count data, referred to below as 'calculated' are reasonably close to the logged data. A detailed review of the data identified the following:

- Both show lower RQD between 20 and 40 m, capturing the effect of near-surface weathering.
- In two sections of the borehole where shale is identified, the logged and calculated RQD and fracture counts diverge.
  - At 80 m the logged RQD is higher than calculated. In this section of core some fault breccia was incorrectly included in RQD length, causing overestimation of the logged value, while the

workflow overestimated aperture, causing underestimation of the calculated value. QA using this process improved the accuracy of the value carried to design.

- A highly sheared bedded sequence between 96 and 102 m has a higher calculated than logged RQD. The discrepancy appears to be caused by the model under-identifying discontinuities in this zone. This may be due to a lack of analogous zones in the training dataset used to develop the model. The shale at this site has a very weak strength along bedding and can be easily broken apart with finger pressure or during drilling. This may also contribute to the difference.

There are many reasons for fracture count estimates to be different: two experienced loggers characterising the same hole may show variation from run to run and discontinuities may open during drilling or be misidentified as mechanical or natural. To validate this tool for use at the project site, a geotechnical practitioner needs to understand systematic under- or over-predictions that the model may make, and account for those in development of the geotechnical model and analysis parameters.

Testing the preliminary model, which was trained with a small dataset (just 110 m of ATV data), provides insight into where the structure picking routine easily replicates physical logging data and where it does not. Improvements to the model are being made by adding training data in a targeted way to address identified gaps and validation of each model update will be completed before implementation. This will allow for rapid development of a workflow that leverages artificial intelligence to speed up standard data processing (structure picking) and to assess geomechanical logging parameters.

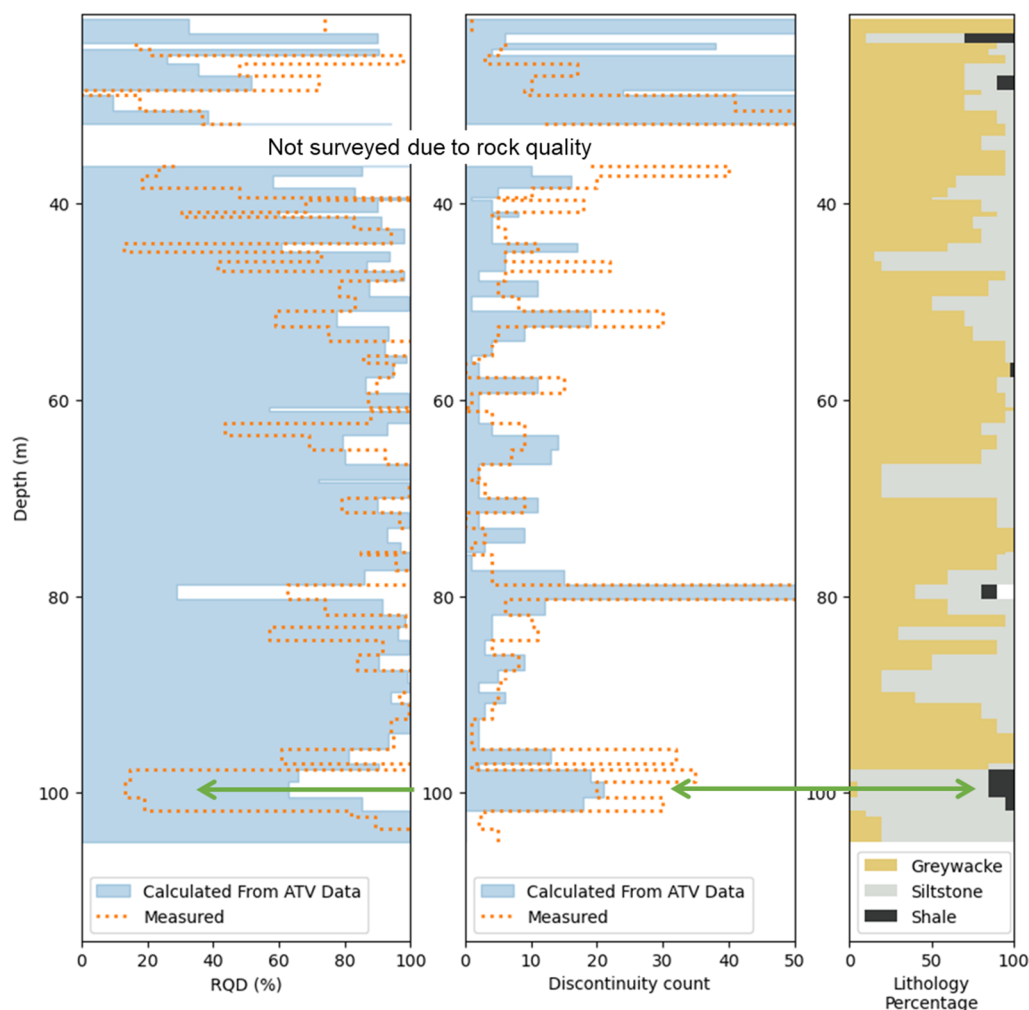


**Figure 14 Automatically estimated RQD and discontinuity counts compared with measured (logged) values and rock type**

## 6 Summary/future work

The workflows presented above have limitations and should not be used alone for characterisation, but they are reliable enough to be effective at identifying logger bias and error, and flagging sections of geotechnical interest for logging within non-geotechnical drilling campaigns. And because they require minutes per hole for processing and plotting, they add significant value for little cost. They provide a means to improve data quality while observing and characterising differences in geotechnical logging data between loggers, programs and consultants.

Additional work is required to improve the performance of the automated logging tool presented above. The tool is based on a preliminary computer vision model developed using a limited training dataset comprising just 110 m of data. It appears to perform well over a range of rock mass conditions but does not account for irregular cracks, tightly-spaced microfractures or sheared bedding that may break upon handling. Model robustness and performance would be improved by increasing the size of the training dataset and by experimenting with different model parameters. It is assumed that the method could be extended to automatic screening of discontinuity type and matching with manual logging data.

At many mines, holes with full geomechanical logging data comprise a small proportion of the televised holes. As automated workflows improve and industry gains experience and confidence in their use, reasonably reliable automated logging of geomechanical parameters like fracture frequency and RQD from ATV data may be possible. Practitioners could then leverage a much larger dataset to develop a more spatially comprehensive geotechnical database for design. The authors suggest that where ATV surveys are completed, an ‘acoustic amplitude’ column be added to geomechanical core logging data table in the site-wide database, whether maintained by owners or consultants. This will allow for future analyses of strength.

## References

- Alzubaidi, F, Mostaghimi, P, Si, G, Swietojanski, P & Armstrong, RT 2022a, ‘Automated rock quality designation using convolutional neural networks’, *Rock Mechanics and Rock Engineering*, vol. 55, no. 6, pp. 3719–3734, <https://doi.org/10.1007/s00603-022-02805-y>.
- Alzubaidi, F, Makuluni, P, Clark, SR, Lie, JE, Mostaghimi, P & Armstrong, RT 2022b, ‘Automatic fracture detection and characterization from unwrapped drill-core images using mask R-CNN’, *Journal of Petroleum Science and Engineering*, vol. 208, Part C, <https://doi.org/10.1016/j.petrol.2021.109471>
- Alzubaidi, F, Nalinakumar, H, Clark, SR, Lie, JE, Mostaghimi, P & Armstrong, RT 2023, ‘Improved fracture segmentation from unwrapped drill-core images using an innovative two-stage segmentation approach’, *Mathematical Geosciences*, <https://doi.org/10.1007/s11004-023-10053-1>.
- Bieniawski, ZT 1976, ‘Rock mass classification in rock engineering’, *Symposium Proceedings of Exploration for Rock Engineering*, pp. 92–106.
- Bu, Y, Song, W, Wang, M & He, Y 2011, ‘The improvement of cementation quality rating method based on compressive strength for low density cement system’, *Procedia Engineering*, vol. 18, pp. 289–294, <https://doi.org/10.1016/j.proeng.2011.11.045>
- Dempers, G, Nguyen, T & Seymour, C 2019, ‘Advanced methodology for geotechnical televiewer interpretation’, *Civil Engineering*, vol. 27, no. 3.
- Gu, W, Bai, S & Kong, L 2022, ‘A review on 2D instance segmentation based on deep neural networks’, *Image and Vision Computing*, vol. 120, <https://doi.org/10.1016/j.imavis.2022.104401>
- Jocher, G, Chaurasia, A & Qiu, J 2023, *YOLO*, version 8.0.0, computer software, Ultralytics, <https://github.com/ultralytics/ultralytics>
- Kao, HC, Chou, PY & Lo, HC 2020, ‘An innovative application of borehole acoustic image and amplitude logs for geotechnical site investigation’, *Acta Geophys*, vol. 68, pp. 1821–1832, <https://doi.org/10.1007/s11600-020-00493-2>.
- Marinos, P & Hoek, E 2000, ‘GSI: A geologically friendly tool for rock mass strength estimation’, *GeoEng 2000*, International Society for Rock Mechanics, pp. 1422–1442.
- Seguin, K, Kinakin, D & Corkum, A 2022, ‘2022 database update – UCS-Leeb hardness correlation’, paper presented at RockEng22: 22nd Canadian Rock Mechanics Symposium, Kingston, 9–10 August 2022.
- Zemanek, J, Glenn, EE, Norton, LJ & Caldwell, RL 1970, ‘Formation evaluation by inspection with the borehole televiewer’, *Geophysics*, vol. 35, no. 2, pp. 254–269.

